Magnetic and multiferroic properties of dilute Fe-doped $BaTiO_3$ crystals

M. Staruch[1], H. ElBidweihy[2], M. G. Cain[3], P. Thompson[4,5], C.A. Lucas[4,5], and P. Finkel[1]

[1]U.S. Naval Research Laboratory, Washington, DC, U.S.A.

[2]U.S. Naval Academy, Annapolis, MD, U.S.A.

[3]Electrosciences Ltd., Farnham, Surrey, U.K.

[4]XMaS Beamline, European Synchrotron Radiation Facility, Grenoble, F-38043, France

[5]Department of Physics, University of Liverpool, Oliver Lodge Laboratory, Liverpool. L69 7ZE. U.K.

Combining and coupling both magnetic and electric properties in one single phase multiferroic material has attracted high interest recently to enable a broad range of novel devices and applications. To evaluate one potential route towards new multiferroics, we have studied 0.5% Fe doped $BaTiO_3$ single crystals and measured the ferroelectric, magnetic, and multiferroic properties. X-ray absorption spectroscopy shows the presence of Fe^{3+}, and magnetic measurements confirmed that this has a significant impact on the magnetic properties. Doping of iron introduces paramagnetism from lone iron atoms as well as what appears to be a weak ferromagnetism. Multiferroicity and magnetoelectric (ME) coupling was observed in the polarization-electric field hysteresis loops with applied magnetic field, yet there was no direct evidence that ME coupling persists when the sample was in the defect dipole-aligned state.

Introduction

$BaTiO_3$ is well known as one of prototypical examples of materials demonstrating ferroelectricity that has a high dielectric constant, low loss tangent and high piezoelectric coefficient (d_{33} ~ 420 pC/N) at room temperature. Interest in doped $BaTiO_3$ (BTO) single crystals has increased in the past decade after seminal results showing that (001) cut and poled crystals doped at the Ti^{4+} site with either Fe^{3+} or Mn^{3+} were shown to have large and recoverable electrostrain of up to 0.8%, significantly higher than the approximately 0.05% which can be obtained reversibly from undoped BTO crystals.[1,2] The improvement in strain is thought to be due to the alignment of defects (i.e. O^{2-} vacancies) with the crystallographic symmetry in the ferroelectric state when the material is aged through application of thermal treatments. This results in the ferroelectric domains favoring alignment with the defect dipoles which provides a restoring force, where recovery of the original ferroelectric domain pattern after non-180º switching results allows for the high strains generated by this reversible domain motion.[3–5]

There is also the possibility that the incorporation of a magnetic ion could give rise to magnetization in these samples and possibly be a new route to creating novel single phase multiferroic materials. Multiferroics demonstrate simultaneous ferroelectric and ferromagnetic properties with coupling between the magnetic and polar order parameters, paving the way for novel memory, sensor, and spintronics devices.[6,7] The possibility of coupling the large strain in these dilutely doped crystals to any magnetic properties remains as yet unexplored. Previous studies of iron doped BTO were focused on very large concentrations, above which the range where the defect dipole behavior is typically observed (x < 2%).[8–11] Room temperature ferromagnetism has previously only been observed for 5% Fe concentrations or higher in $BaTiO_3$ single crystals,[8] but other studies on nanostructures or bulk materials have shown ferromagnetism in concentrations as low as 1% molar concentration of Fe[9]. In the ceramic

samples, oxygen vacancies were theorized to facilitate a superexchange interaction between nearest neighbor Fe^{3+} ions. But overall it is still controversial to attribute any ferromagnetic (FM) loops to the doped BTO and not secondary phases or other factors. Iron doping is also known to promote the formation of a hexagonal $P6_3/mmc$ phase, and this may be the result of some discrepancies between paramagnetism and ferromagnetism observed for dilutely doped samples in the literature.[12–14]

However, very few studies on the multiferroic properties of these materials are present in the literature, in part due to the decrease in polarization and subsequent disappearance of the ferroelectric ordering with increasing amounts of the transition metal dopant. The only work on Mn doped BTO with similar dopant concentrations (0.5 – 2%) to have looked at the multiferroicity have not looked at the coupling[15] or have found the magnetism and ferroelectricity were decoupled[16]. It is therefore the goal of this work to both evaluate the magnetism that is present in 0.5% Fe doped BTO single crystals, as well as any potential of the material to be used as a single phase multiferroic.

Experimental Techniques

(001) oriented and poled $BaTi_{0.995}Fe_{0.005}O_3$ (BTFO) and undoped BTO crystals were provided by Ceracomp Co. Ltd. using a solid-state single crystal growth (SSCG) method. This method is described in more detail in Ref. 17. The as-received samples were aged at 80°C in air for 24 hours to allow for diffusion and defect dipole formation. Ferroelectric and piezoelectric testing was done with a home-built Sawyer-Tower system. X-ray absorption spectroscopy was carried out on the XMaS beamline (BM28), at the European Synchrotron Radiation Facility, in Grenoble. Magnetic measurements as a function of temperature and magnetic field were performed using a vibrating sample magnetometer (VersaLab, Quantum Design) with operating

temperature 50 K – 400 K and magnetic fields up to 3 T (30,000 Oe). Using the VersaLab, connections were also made to a LCR meter for magnetocapacitance measurements. Sample crystallography was calculated using Rietveld refinement (GSAS II)[18] from diffraction data generated from a crushed sample set spinning in the ID22, High Resolution Powder Diffraction beamline, ESRF. Ferroelectric polarization/electric field measurements (PE Loops) were carried out at the XMaS beamline, ESRF, using a capability recently developed for in situ and in operando x-ray diffraction measurements [see refs. [19,20]]. The system can be used independently to acquire ferroelectric polarisation with electric field as a function of temperature and applied magnetic field, details of which may be found at www.xmas.ac.uk [ref. [21]]. A static magnetic field of up to 3T was applied in the direction of polarization and counter to that direction and the resulting PE loop was measured to discern any differences in ferroelectric behavior as a function of applied external magnetic field.

Results and Discussion

After aging, the ferroelectric and piezoelectric properties of the sample were measured. A pinched hysteresis loop and recoverable large strain were observed, consistent with previous reports. However, it is important to note that after several electric field cycles, the pinching disappeared and the strain significantly decreased. Overall, with repeated application of the electric field, the ferroelectric properties moved towards those of an undoped BTO crystal. This suggests that the electric field allows for migration of the oxygen vacancies in the sample and therefore the defect dipole alignment to the ferroelectric dipole moments is not maintained. It was also found that the original behavior shown in Figure 1 can always be recovered through the completion of another aging process, so the material may be re-set. Further investigation into this

phenomenon is currently ongoing, but it is important to note when discussing the magnetic and multiferroic properties that the sample is expected to be very sensitive to the prehistory.

The current samples were confirmed to be fully tetragonal (P4mm) by room temperature powder x-ray diffraction as shown in Supplemental Information Figure S1(a), with Rietveld refined parameters: Rw=20.0%, a=b= 3.99499Å, c=4.03634Å. No secondary phase of ferrite Fe (Imax=(110) at 2ϑ=10.023º) or austenite Fe (Imax=(111) at 2ϑ=9.866º) was observed at experimental detection levels of ~ about 0.5% based on the detection of lowest intensity BTO reflection (900). No preferred orientation in the tetragonality was observed in the diffraction data, as expected from crushed material and set spinning in the x-ray beam. The incorporation of 0.5at% Fe on either the Ba site or the Ti site does not significantly affect or impact the Rietveld refinement of the x-ray diffraction data. X-ray absorption spectroscopy on the BTFO sample confirms the presence of iron as shown in Figure 2, and the position of the iron edge as compared to several reference samples suggests that the iron is in the 3+ oxidation state (Fe^{3+}). This is as expected based on previous reports and is consistent with the charge deficiency that would allow for the formation of oxygen vacancies and defect dipoles. While the pre-edge feature is not as sharp as the references, it is strongly dependent on site symmetry and may actually indicate a non-centrosymmetric position which could suggest a local polar moment extends to the Fe^{3+} sites as well.[22]

Zero field cooled (ZFC) and field cooled (FC) magnetization versus temperature data are plotted in Figure 3(a) and (b) for the BTO and BTFO crystals, respectively. The BTO sample shows predominantly diamagnetism, with the exception of a paramagnetic contribution that becomes dominant at low temperatures. This is consistent with what would be expected for a bulk BTO sample.[23] However, with 1 T applied magnetic field, two distinct anomalies appear in

the nominally undoped BTO crystal at 111 K and 252 K which do not correspond to any of the structural phase transitions of BTO. Instead, these most likely correspond to very small amounts of iron oxide impurity phases, corresponding to the Verwey transition in Fe_3O_4 and the antiferromagnetic (AFM) to canted AFM transition in Fe_2O_3, respectively. In fact, processing of Fe_2O_3 at high temperatures can lead to the mixture of these phases and has also been shown to slightly decrease the Verwey transition temperature as observed here.[24] The presence of these phases is also most likely what causes the split of the ZFC and FC curves for the 0.5 T data as well. Although iron impurities in nominally undoped samples have previously been reported,[1] it should be noted that the present undoped crystal does not show any defect dipole behavior, which would also be consistent with the iron forming as a small amount of secondary phase. Beyond this, though, the diamagnetic response of BTO itself is the predominant contribution to the signal.

In contrast to the curves for undoped BTO, the BTFO sample does not show any magnetic anomalies related to iron oxide impurity phases as shown in Figure 3(b). This is consistent with no detection of secondary phases in the powder diffraction data [Supplemental Fig. S1(b)], and in fact magnetic measurements are also highly sensitive to the presence of any magnetic impurity phases so the absence of the signatures observed in the undoped sample confirm that the iron is incorporated into the BTO lattice. Although there is a slight diamagnetic contribution seen in the negative magnetization values at higher temperatures with 1 T applied field, the dominating contribution to the magnetic signal is paramagnetic. The absence of any divergence of the ZFC and FC curves also disallows for superparamagnetic particle clusters in the sample, again suggesting the absence of any impurity phase in the BTFO crystal. The paramagnetism seems likely to arise from the interactions of distant iron ions dispersed in the

matrix in this dilutely doped sample. This is consistent with a previous report of $BaTiO_3$ doped with Co, Fe, and Cr (between 1.5% and 3.5%) showing paramagnetism at all temperatures measured that was also thought to originate from the transition metal ions.[25] No anomalies are present in the derivative of the M vs. T data that would otherwise suggest magnetic ordering within the range of temperatures measured.

Magnetization versus magnetic field data were also recorded at multiple temperatures and selected curves are plotted in Figure 4(a). Here it is instructive to note that even though there is no evidence of ferromagnetism in the M vs. T data that all of the curves have an S-shape with some small opening of the hysteresis loop. This is the case for both the BTO and the BTFO sample, and could be consistent with other reports of surface oxygen or oxygen vacancies and other defects in the lattice.[26,27] Yet once the paramagnetic or diamagnetic background is subtracted from these curves, we can see that there is no temperature dependence evident in the data for undoped BTO whereas there is a temperature evolution of the saturation magnetization (M_S) that indicates a weak ferromagnetic ordering in the BTFO sample as shown in Figure 4(b). Extrapolating the change in M_S with temperature to reach the temperature-independent value of undoped BTO, this would suggest a Curie temperature (T_C) of 550 – 600 K assuming a power law dependence [$M \propto (T_C - T)^{\beta}$] with the critical exponent β~0.5.[28,29] This could explain why no evidence of this transition is observed in the magnetization versus temperature data, as we did not go up above T_C during the measurements which would show the best evidence of this weak FM moment.

The values of M_S are extremely low (~0.01 μ_B/Fe), suggesting any long-range order is very weak. In that respect the magnetism here is very different from the very high moments observed in the dilute magnetic semiconductors,[30,31] so any FM interactions in the present sample

are most likely not due to the formation of impurity bands or magnetic polarons as have been proposed for those systems as well as a 0.5% Mn doped BTO that also showed orders of magnitude higher magnetization that was explained through bound polarons[15]. The magnetic polaron model accounts for the localization of the electron associated with a charged defect complex, in this present case the singly charged $Fe'_{Ti} - V_O^{\cdot\cdot}$. The BTFO crystal would be expected to have defect concentrations below that allowing for double exchange mitigated through oxygen vacancies, and appears to be close to or below the critical doping level for significant overlap of hydrogenic orbitals that would result in percolation of strong long range ordering. It appears most likely that most of the Fe^{3+} are isolated and contribute Pauli paramagnetism, but there is the formation of some long range ordering potentially through the formation of magnetic polarons. Future work on samples with higher dopant concentration is currently planned to look for stronger ferromagnetic ordering while maintaining defect dipole behavior.

Lastly, as there is some evidence of a weak FM ordering, it is important to evaluate the multiferroic coupling. Capacitance versus temperature measurements with and without applied magnetic fields were made directly after the sample was re-aged. It should be noted that the capacitance magnitude includes stray capacitance and is not the absolute value of the samples. In addition, ferroelectric hysteresis loops were measured with an applied magnetic field, and both these results are shown in Figure 5. In the magnetocapacitance measurements, even at fields of up to 3 T there is no difference in capacitance with temperature. However, there is a statistically significant change in the ferroelectric response with applied magnetic field, notably in the material's electric coercive field E_C which seems to contradict the capacitance measurements. It's important to note that there is no pinching in the ferroelectric hysteresis loop though, suggesting

that this sample has been de-aged leaving no net defect dipole alignment and therefore no longer any enhanced piezoelectricity. However, for the magnetocapacitance measurement, the sample was aged immediately prior to measurement and hence left in a stable polarization state. The two measurements differ in another important way: the ferroelectric measurement is a large field measurement whilst the capacitance measurement is that for a minor loop (1 V applied over 1 mm), and thus magnetocapacitance measurements without a bias electric field near E_C is not likely to capture any evidence of multiferroicity. Near E_C, the magnetoelectric (ME) coupling coefficient $\alpha = dP/dH$ (the derivative of polarization P with respect to applied magnetic field H) is within the range of other single phase multiferroic materials with a maximum value of $\alpha_{ME} = 2.3 \times 10^{-9}$ s/m. However, while non-zero, α_{ME} is considerably smaller at zero electric field. We must also consider the possibility that the presence of defect dipoles is incompatible with multiferroic behavior in this sample. To the best of our knowledge, there are no reports showing the coexistence of these phenomena and the only previous reports on multiferroicity do not measure or they explicitly state that there is zero magnetoelectric coupling.[15,16] Further study of these crystals with defect dipole alignment are necessary to evaluate if we would be able to tune the extraordinarily high 0.8% strains with a remote magnetic field.

Conclusion

In summary, undoped $BaTiO_3$ and 0.5% Fe doped $BaTiO_3$ single crystals were aged and the ferroelectric, magnetic, and multiferroic properties measured. After aging, pinched electric hysteresis loops were observed as well as large strains up to 0.8%. The introduction of Fe^{3+} as confirmed by x-ray absorption spectroscopy had a significant impact on the magnetic properties, introducing paramagnetism from lone iron spins as well as what appears to be a weak ferromagnetism. Although evidence of multiferroicity and magnetoelectric coupling was

observed in the PE loops with applied magnetic field, there is not yet direct evidence that the ME nature can coexist with the defect dipole-aligned aged state of the crystal.

Supplementary Material

See supplementary material for the powder x-ray diffraction and Rietveld refinement of a crushed iron doped $BaTiO_3$ sample.

Acknowledgments

The authors would like to acknowledge funding from the Office of Naval Research under the U.S. Naval Research Laboratory's Basic Research Program, and Office of Naval Research Global, ONRG - NICOP Project Number: N62909-18-1-2008 Electrosciences Ltd.. Parts of this research work was carried in the framework of the ADVENT project (Grant Number: 16ENG06 ADVENT) which is supported by the European Metrology Programme for Innovation and Research (EMPIR). The EMPIR initiative is co-funded by the European's Horizon 2020 research and innovation programme and the EMPIR Participating States. Andy Fitch from ID22, ESRF performed the powder diffraction, and Mark Newton, ESRF (now ETZ, Zurich) analysed some of the XAS data.

References

[1] X. Ren, *Large electric-field-induced strain in ferroelectric crystals by point-defect-mediated reversible domain switching*, Nat. Mater. **3**, 91 (2004).

[2] L.X. Zhang and X. Ren, *In situ observation of reversible domain switching in aged Mn-doped BaTiO 3 single crystals*, Phys. Rev. B **71**, 174108 (2005).

[3] E. Burcsu, G. Ravichandran, and K. Bhattacharya, *Large strain electrostrictive actuation in barium titanate*, Appl. Phys. Lett. **77**, 1698 (2000).

[4] S.-E. Park, S. Wada, L.E. Cross, and T.R. Shrout, *Crystallographically engineered BaTiO3 single crystals for high-performance piezoelectrics*, J. Appl. Phys. **86**, 2746 (1999).

[5] Y. Zhang, J. Li, and D. Fang, *Oxygen-vacancy-induced memory effect and large recoverable strain in a barium titanate single crystal*, Phys. Rev. B **82**, 064103 (2010).

[6] M. Bibes and A. Barthélémy, *Multiferroics: towards a magnetoelectric memory.*, Nat. Mater. **7**,

425 (2008).

[7] W. Eerenstein, N.D. Mathur, and J.F. Scott, *Multiferroic and magnetoelectric materials*, Nature **442**, 759 (2006).

[8] S. Ray, P. Mahadevan, S. Mandal, S.R. Krishnakumar, C.S. Kuroda, T. Sasaki, T. Taniyama, and M. Itoh, *High temperature ferromagnetism in single crystalline dilute Fe-doped BaTiO3*, Phys. Rev. B **77**, 104416 (2008).

[9] K.C. Verma, V. Gupta, J. Kaur, and R.K. Kotnala, *Raman spectra, photoluminescence, magnetism and magnetoelectric coupling in pure and Fe doped BaTiO3 nanostructures*, J. Alloys Compd. **578**, 5 (2013).

[10] S. QIU, W. LI, Y. LIU, G. LIU, Y. WU, and N. CHEN, *Phase evolution and room temperature ferroelectric and magnetic properties of Fe-doped BaTiO3 ceramics*, Trans. Nonferrous Met. Soc. China **20**, 1911 (2010).

[11] B. Xu, K.B. Yin, J. Lin, Y.D. Xia, X.G. Wan, J. Yin, X.J. Bai, J. Du, and Z.G. Liu, *Room-temperature ferromagnetism and ferroelectricity in Fe-doped BaTiO3*, Phys. Rev. B **79**, 134109 (2009).

[12] F. Lin, D. Jiang, X. Ma, and W. Shi, *Influence of doping concentration on room-temperature ferromagnetism for Fe-doped BaTiO3 ceramics*, J. Magn. Magn. Mater. **320**, 691 (2008).

[13] B. Deka, S. Ravi, A. Perumal, and D. Pamu, *Ferromagnetism and ferroelectricity in Fe doped BaTiO3*, Phys. B Condens. Matter **448**, 204 (2014).

[14] N. V. Dang, T.D. Thanh, L. V. Hong, V.D. Lam, and T.-L. Phan, *Structural, optical and magnetic properties of polycrystalline BaTi 1−x Fe x O 3 ceramics*, J. Appl. Phys. **110**, 043914 (2011).

[15] Y.-H. Lin, J. Yuan, S. Zhang, Y. Zhang, J. Liu, Y. Wang, and C.-W. Nan, *Multiferroic*

behavior observed in highly orientated Mn-doped BaTiO3 thin films, Appl. Phys. Lett. **95**, 033105 (2009).

[16] J.Y. Son, J.-H. Lee, S. Song, Y.-H. Shin, and H.M. Jang, *Four-States Multiferroic Memory Embodied Using Mn-Doped BaTiO 3 Nanorods*, ACS Nano **7**, 5522 (2013).

[17] S.-J.L. Kang, J.-H. Park, S.-Y. Ko, and H.-Y. Lee, *Solid-State Conversion of Single Crystals: The Principle and the State-of-the-Art*, J. Am. Ceram. Soc. **98**, 347 (2015).

[18] B.H. Toby and R.B. Von Dreele, *GSAS-II : the genesis of a modern open-source all purpose crystallography software package*, J. Appl. Crystallogr. **46**, 544 (2013).

[19] M.G. Cain, editor , *Characterisation of Ferroelectric Bulk Materials and Thin Films* (Springer Netherlands, Dordrecht, 2014).

[20] C. Vecchini, P. Thompson, M. Stewart, A. Muñiz-Piniella, S.R.C. McMitchell, J. Wooldridge, S. Lepadatu, L. Bouchenoire, S. Brown, D. Wermeille, O. Bikondoa, C.A. Lucas, T.P.A. Hase, M. Lesourd, D. Dontsov, and M.G. Cain, *Simultaneous dynamic electrical and structural measurements of functional materials*, Rev. Sci. Instrum. **86**, 103901 (2015).

[21] P.B.J. Thompson, S.D. Brown, L. Bouchenoire, D. Mannix, D.F. Paul, C.A. Lucas, J. Kervin, M.J. Cooper, P. Arakawa, and G. Laughon, in *AIP Conf. Proc.* (AIP, 2007), pp. 1683–1686.

[22] M.-A. Arrio, S. Rossano, C. Brouder, L. Galoisy, and G. Calas, *Calculation of multipole transitions at the Fe K pre-edge through p-d hybridization in the Ligand Field Multiplet model*, Europhys. Lett. **51**, 454 (2000).

[23] R.V.K. Mangalam, N. Ray, U. V. Waghmare, A. Sundaresan, and C.N.R. Rao, *Multiferroic properties of nanocrystalline BaTiO3*, Solid State Commun. **149**, 1 (2009).

[24] R. Aragón, D.J. Buttrey, J.P. Shepherd, and J.M. Honig, *Influence of nonstoichiometry on the Verwey transition*, Phys. Rev. B **31**, 430 (1985).

[25] H. Liu, B. Cao, and C. O'Connor, *Intrinsic magnetism in BaTiO 3 with magnetic transition element dopants (Co, Cr, Fe) synthesized by sol-precipitation method*, J. Appl. Phys. **109**, 07B516 (2011).

[26] L. Yang, H. Qiu, L. Pan, Z. Guo, M. Xu, J. Yin, and X. Zhao, *Magnetic properties of BaTiO3 and BaTi1−xMxO3 (M=Co, Fe) nanocrystals by hydrothermal method*, J. Magn. Magn. Mater. **350**, 1 (2014).

[27] S. Qin, D. Liu, Z. Zuo, Y. Sang, X. Zhang, F. Zheng, H. Liu, and X.-G. Xu, *UV-Irradiation-Enhanced Ferromagnetism in BaTiO 3*, J. Phys. Chem. Lett. **1**, 238 (2010).

[28] J.H. Hildebrand, *The "Critical Point"* (CRC Press, 1952).

[29] H.E. Stanley, *Introduction to Phase Transitions and Critical Phenomena* (Oxford University Press, 1971).

[30] J.M.D. Coey, *High-temperature ferromagnetism in dilute magnetic oxides*, J. Appl. Phys. **97**, 10D313 (2005).

[31] J.M.D. Coey, M. Venkatesan, and C.B. Fitzgerald, *Donor impurity band exchange in dilute ferromagnetic oxides*, Nat. Mater. **4**, 173 (2005).

Figure Captions:

Figure 1. (a) Polarization and (b) strain vs. electric field for the doped BTO crystal.

Figure 2. X-ray absorption spectra showing the normalized absorbance of the Fe doped BTO crystal as compared to reference samples.

Figure 3. Zero field cooled and field cooled magnetization vs. temperature curves for (a) undoped BTO crystal and (b) 0.5% Fe doped BTO crystal. The red and black curves are with 0.5 T and 1 T applied field, respectively.

Figure 4. Magnetization vs. magnetic field for doped and undoped BTO samples. (b) Temperature dependence of the corrected magnetization vs. magnetic field loops for the doped BTO sample (all paramagnetic or diamagnetic contributions subtracted). The inset shows the temperature dependence of the saturation magnetization, and the extrapolation to the Curie temperature.

Figure 5. (a) Capacitance and tanδ vs. temperature and (b) polarization vs. electric field curves at 0 T and (±)3 T applied magnetic fields. The inset of part (b) shows the full hysteresis loop.

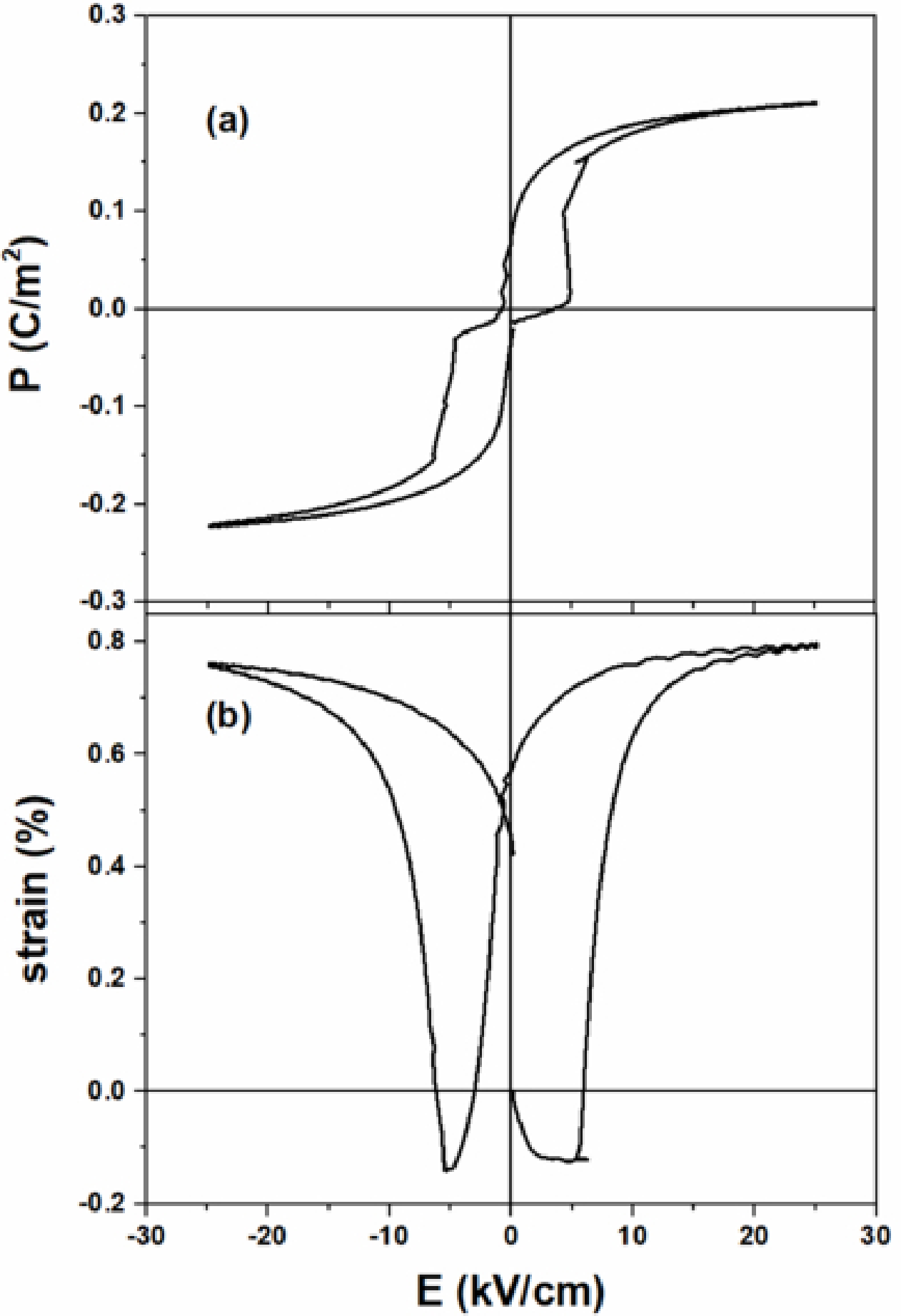
(a)
(b)
P (C/m^2)
strain (%)
E (kV/cm)
0.3
0.2
0.1
0.0
-0.1
-0.2
-0.3
0.8
0.6
0.4
0.2
0.0
-0.2
-30
-20
-10
0
10
20
30

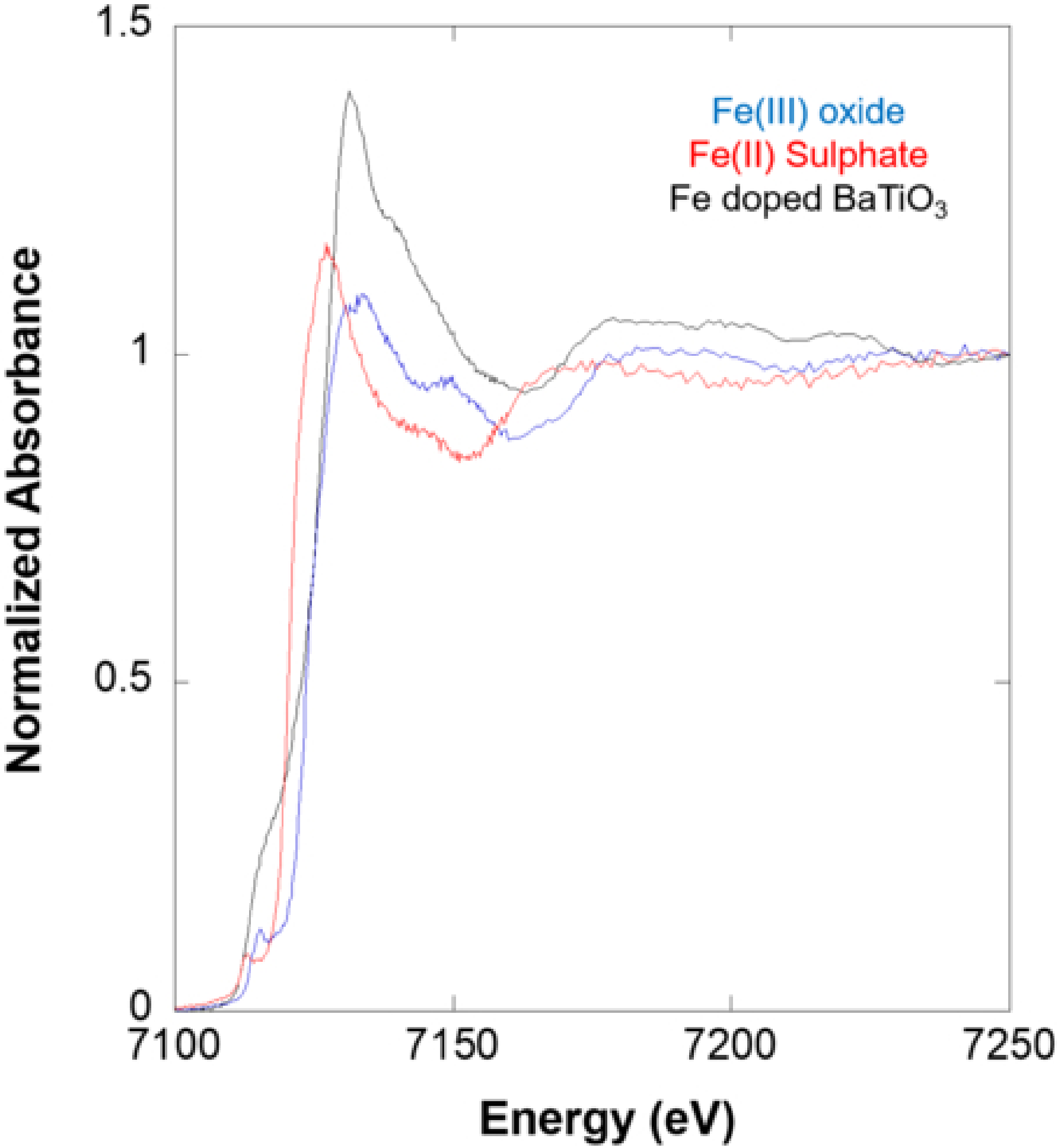
1.5
1
0.5
0
Normalized Absorbance
7100
7150
7200
7250
Energy (eV)
Fe(III) oxide
Fe(II) Sulphate
Fe doped BaTiO3

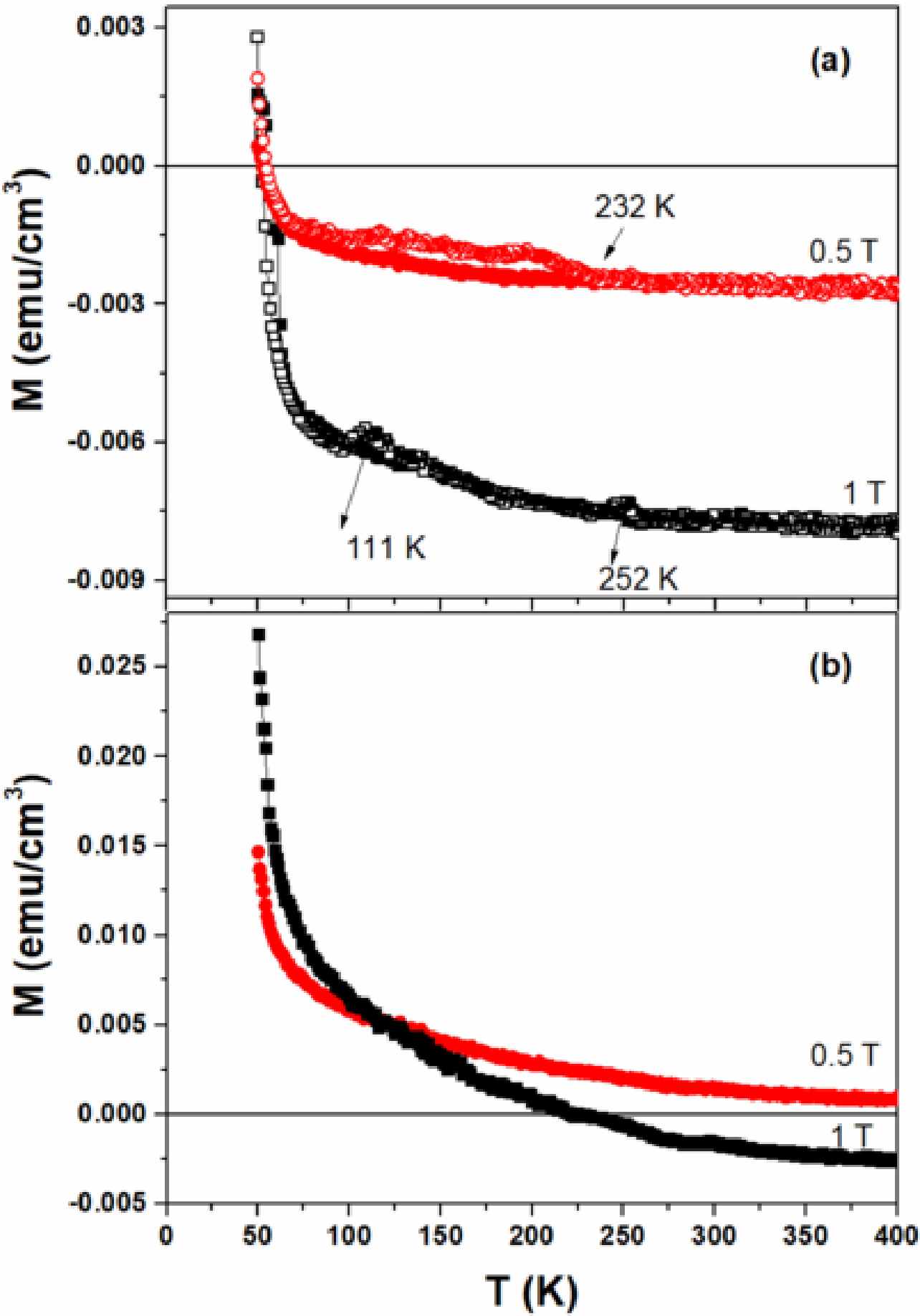
(a)
0.003
0.000
-0.003
-0.006
-0.009
M (emu/cm^3)
232 K
0.5 T
1 T
111 K
252 K
(b)
0.025
0.020
0.015
0.010
0.005
0.000
-0.005
M (emu/cm^3)
0.5 T
1 T
0
50
100
150
200
250
300
350
400
T (K)

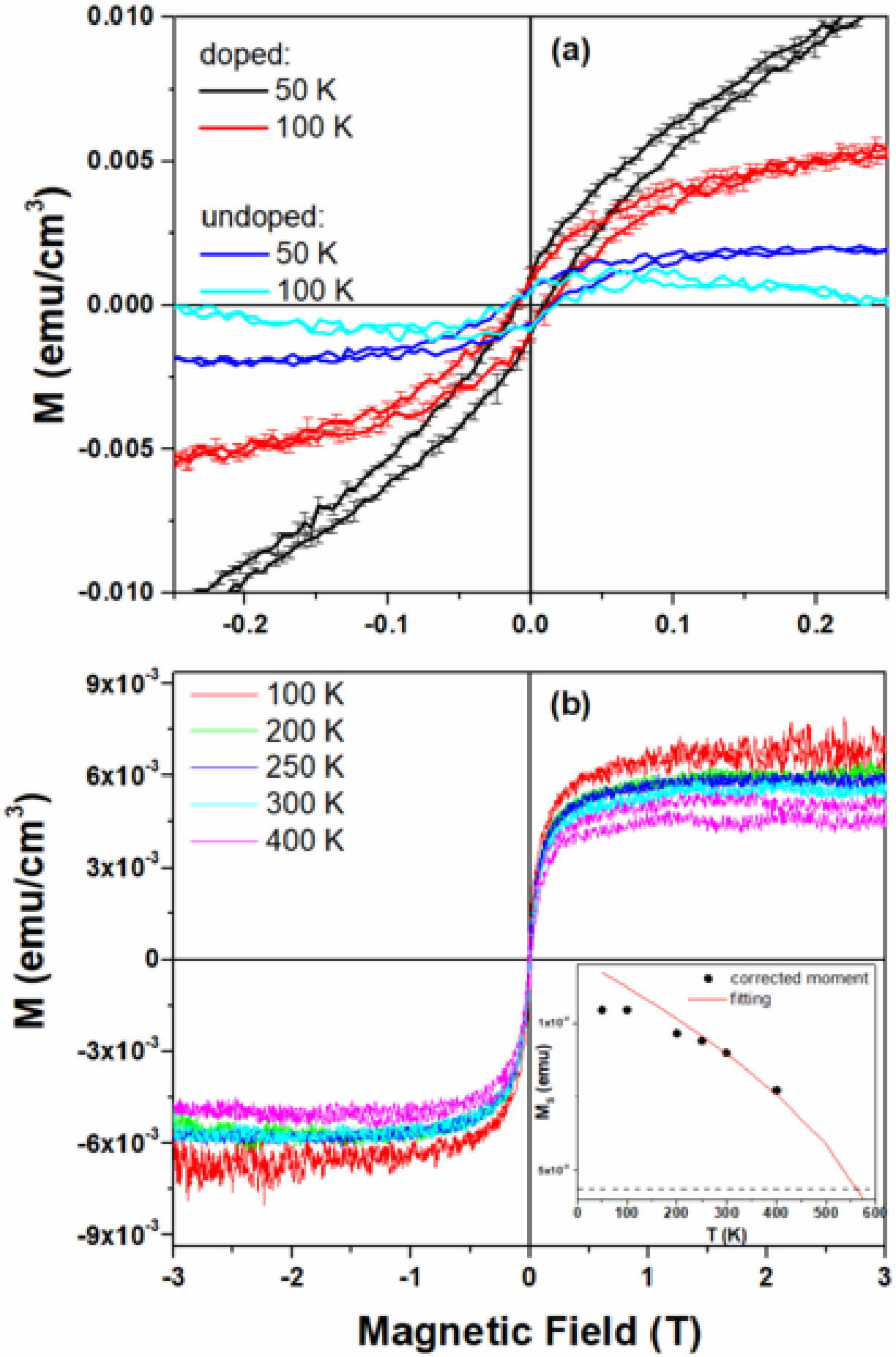
(a)
doped:
50 K
100 K
undoped:
50 K
100 K
M (emu/cm^3)
0.010
0.005
0.000
-0.005
-0.010
-0.2
-0.1
0.0
0.1
0.2
(b)
100 K
200 K
250 K
300 K
400 K
M (emu/cm^3)
9x10^{-3}
6x10^{-3}
3x10^{-3}
0
-3x10^{-3}
-6x10^{-3}
-9x10^{-3}
-3
-2
-1
0
1
2
3
Magnetic Field (T)
corrected moment
fitting
M$_s$ (emu)
T (K)
0
100
200
300
400
500
600

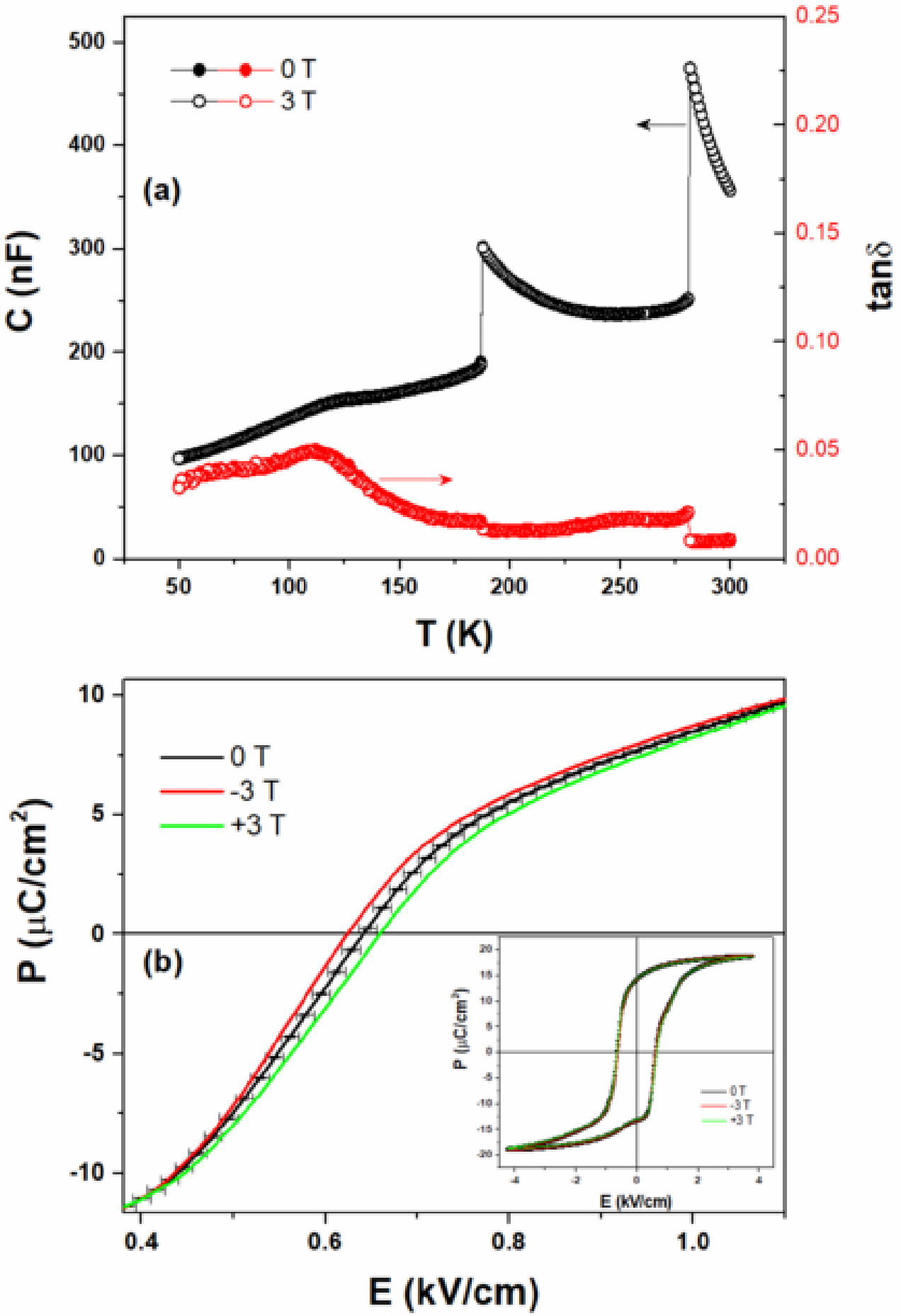
0 T
3 T
(a)
C (nF)
tanδ
T (K)
0 T
-3 T
+3 T
(b)
P (μC/cm²)
E (kV/cm)
P (μC/cm²)
E (kV/cm)